Chapter 2
Germanene on Pt(111)

Abstract The tremendous progress in graphene research has motivated us to investigate analogous 2D crystalline systems—new two-dimensionally ordered materials composed of elements other than carbon. Here, this chapter presents the fabrication and structural characterization of germanene on a Pt(111) surface, which is the germanium-based counterpart of graphene. LEED and STM, combined with density functional theory (DFT)-based ab initio calculations reveal the buckled honeycomb-like structure of Pt-supported germanene. Calculated electron localization function (ELF) demonstrates the continuity of 2D germanene on Pt(111).

Keywords Germanene · Germanium · STM · LEED · Honeycomb structure · Pt(111)

2.1 Background

2.1.1 From Silicene to Germanene

The explosive studies on graphene have aroused significant interests towards other graphene-like single-element 2D materials. Graphene is derived from the group IV elements, so it is natural to consider the possibility of graphene analogs based on other group IV elements, such as silicon and germanium. However, silicon and germanium are known to favor sp^3-hybridized, tetrahedral bonds in contrast to planar sp^2 hybridization in graphite. So single layers of silicon and germanium, so-called silicene and germanene, cannot be derived directly from their bulk counterparts. Instead, they have first been fabricated from the computational side. First-principles calculations demonstrated free-standing silicene and germanene favor to adopt a low-buckled honeycomb structure, forming a mixed sp^2–sp^3 like hybridized state [1]. Further theoretical calculations revealed that epitaxial silicene (germanene) on substrates possesses a bandgap of 1.55 meV (23.9 meV) due to the symmetry-breaking and enhanced spin-orbital coupling effects. In particular, a quantum spin Hall effect was predicted in buckled germanene [2], and high-T_c superconductivity was anticipated in doped germanene [3] (where T_c represents the critical temperature for

L. Li, *Fabrication and Physical Properties of Novel Two-dimensional Crystal Materials Beyond Graphene: Germanene, Hafnene and $PtSe_2$*, Springer Theses,
https://doi.org/10.1007/978-981-15-1963-5_2

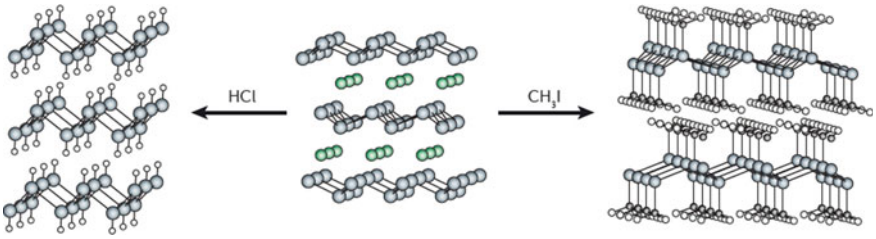

Fig. 2.1 Synthesis of germanane and methylated germanane. Reproduced with permission from Ref. [6], © 2015 ACS; [5], © 2014 Springer Nature

superconductivity). These properties indicate potential applications of silicene and germanene in electronics, spintronics, and photonic devices.

The synthesis of silicene and germanene is the primary step towards the realization of their exotic properties and potential applications. Lack of layered bulk analogs necessitates "bottom-up" growth method, i.e., deposition of silicene and germanene on substrates. The exploration of epitaxial growth of silicon on silver surfaces resulted in the formation of Si nanowires on Ag(100), Si nanoribbons on Ag(110), and silicene on Ag(111). Later, additional studies have reported the fabrication of silicene on Ir(111), ZrB_2 and MoS_2, as discussed in Chap. 1.

2.1.2 Early Exploration of Germanene Growth

The preliminary studies of germanene growth started with solution-based exfoliation processes [4]. Chemically treating $CaGe_2$ in HCl created hydrogenated germanene [5], that is, germanane (GeH). Further investigations yielded methylated germanane by treating $CaGe_2$ in CH_3I [6, 7], as depicted in Fig. 2.1. These functionalized germanene sheets showed strong oxidation resistance in ambient conditions. However, these Ge–H and Ge–CH_3 bonds enhance the sp^3 hybridization of Ge atoms, which disables 2D honeycomb structures resulting from sp^2-hybridized orbitals, and more essentially, the linear dispersion relation at the Dirac point. Therefore, these layered materials are not germanene in nature. To the best of our knowledge, the actual fabrication of germanene has not yet been reported, which is our research background and motivation.

2.2 Fabrication and Computation Methods

We grow single-layer germanene sheets on a Pt(111) substrate by surface-assisted molecular beam epitaxial (MBE) [8], as illustrated in Fig. 2.2. The choice of a Pt(111) substrate is based on several advantageous characteristics of Pt(111), such

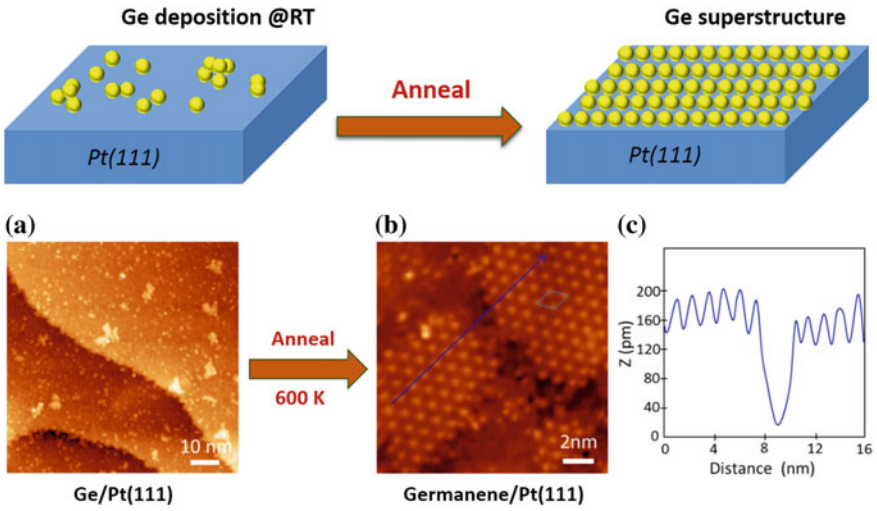

Fig. 2.2 Upper: schematic illustration of physical vapor deposition of germanene on Pt(111). Lower: **a** STM topography of Ge deposited on Pt(111) at room temperature. **b** Ge superstructures formed after annealing at 600 K. **c** The line profile along the blue line in (**b**) showing the thickness of single-layer germanene

as its hexagonal symmetry serving as a growth template and its weaker interfacial interaction with adsorbed 2D honeycomb sheets (e.g. graphene) relative to other metals [9, 10]. Experiments were performed in an ultra-high vacuum (UHV) system with a base pressure of about 2×10^{-10} mbar. The Pt(111) surface was cleaned by several cycles of sputtering and annealing until it yielded distinct Pt(1×1) diffraction spots in the LEED pattern and clean surface terraces in the STM images. The germanium was evaporated onto the Pt(111) substrate kept at room temperature from a high-purity Ge rod mounted in an electron-beam evaporator. The amorphous surface covered by Ge particles and clusters was observed in Fig. 2.2a. The sample was then annealed at a temperature range of 600–750 K for 30 min, which was below 800 K for the sake of excluding the formation of a Ge–Pt surface alloy. STM was then employed to characterize the as-prepared Ge superstructures, as shown in Fig. 2.2b, c. LEED was utilized to identify the superstructures macroscopically.

Our DFT-based first-principle calculations were performed using the Vienna ab initio simulation package (VASP) [11, 12]. The projector augmented wave (PAW) potentials were used to describe the core electrons, and the local density approximation (LDA) was used for exchange and correlation [13]. The periodic slab models included four layers of Pt, one layer of germanium, and a vacuum layer of 15 Å. All atoms were fully relaxed except for the bottom two substrate layers until the net force on every atom was less than 0.01 eV/Å. The energy cutoff of the plane-wave basis sets was 400 eV, and the K-points sampling was $3 \times 3 \times 1$, generated automatically with the origin at the Γ-point.

2.3 Structural Characterizations and Theoretical Calculations

The structure of the germanium layer formed on the Pt(111) surface is characterized macroscopically by LEED, as shown in Fig. 2.3. The six outer symmetric bright spots can be assigned to the pristine Pt(111) substrate, which has a six-fold symmetry. The additional distinct diffraction spots originate from the germanium superstructures. For clarity, we sketched a map of the diffraction spots of the superstructure in reciprocal space (Fig. 2.3b), where the reciprocal vectors of each group of spots are indicated by differently colored arrows. Aside from the (1×1) diffraction spots of the Pt(111) lattice, two symmetrically equivalent domains exist, identified by red and blue spots, respectively. Aiming to understand this LEED pattern more thoroughly, a schematic diagram in real space consistent with the diffraction patterns is provided in Fig. 2.3c. This diagram directly reveals the commensurable relation between the germanium adlayer and the substrate lattice. Germanium forms a superstructure with matrix $\begin{bmatrix} 2 & -3 \\ 3 & 5 \end{bmatrix}$ or the equivalent $\begin{bmatrix} 3 & -2 \\ 2 & 5 \end{bmatrix}$ and the corresponding angles between the close-packed direction of Pt[1 $\bar{1}$ 0] and this superstructure can be obtained as 36.6° and 23.4°, respectively. From the data, this superstructure can be easily identified as a $(\sqrt{19} \times \sqrt{19})$ superstructure with respect to the Pt(111) substrate.

In order to characterize the germanium adlayer in detail, we subsequently carried out STM measurements. The large-scale STM image in Fig. 2.4a shows the long-range order of the germanium superstructure formed on the Pt(111) surface. One of the supercells is marked by the blue rhombus. The orientation of the supercell is rotated about 23° relative to Pt[1 $\bar{1}$ 0] direction. The corresponding high-resolution

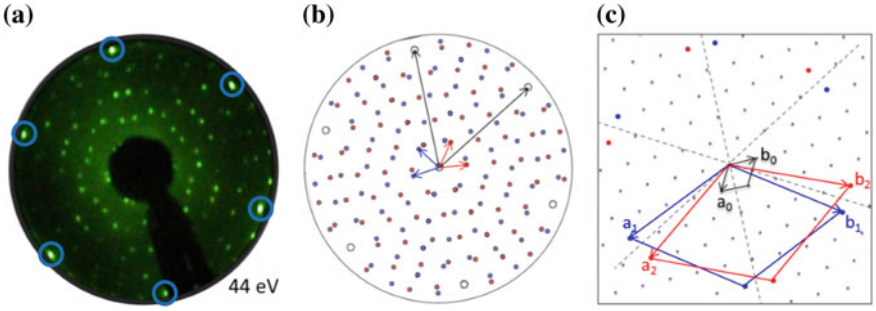

Fig. 2.3 LEED patterns and the corresponding schematic diagram of the germanium superstructure formed on the Pt(111) surface. **a** The six outer spots indicated by circles originate from the six-fold symmetry of the Pt(111) substrate. The additional diffraction spots are ascribed to the germanium adlayer. **b** Schematic representation of the diffraction spots shown in (**a**), where the reciprocal vectors of each group of spots are indicated by black, red, or blue arrows. **c** Schematic diagram of the diffraction spots in real space. These data reveal a $(\sqrt{19} \times \sqrt{19})$ superstructure of the germanium layer [lattice vectors (a_1, b_1) or (a_2, b_2)] with respect to the Pt(111) lattice [lattice vectors (a_0, b_0)]. Reprinted with permission from Ref. [8], © 2014 Wiley

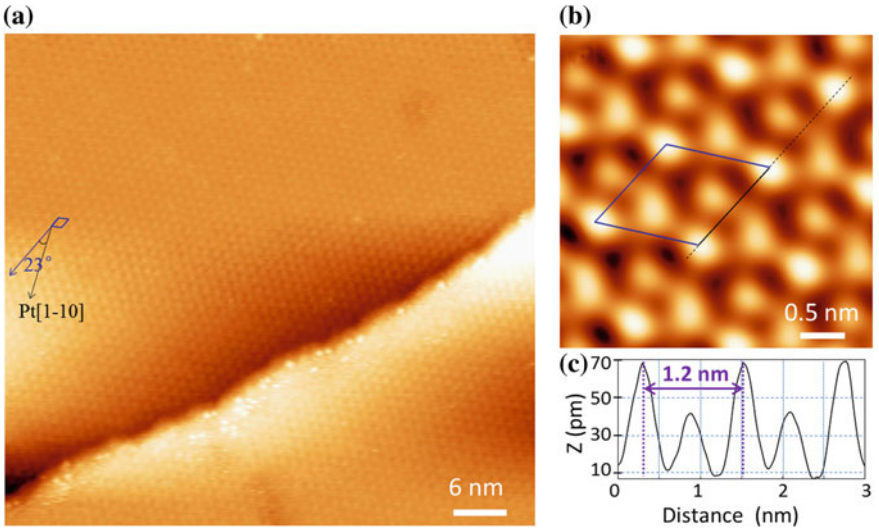

Fig. 2.4 **a** Occupied-state STM image (U = −1.45 V, I = 0.25 nA), showing a ($\sqrt{19} \times \sqrt{19}$) superstructure of the germanium adlayer formed on the Pt(111) surface. The direction of this reconstruction is indicated by the blue arrow. The close-packed direction Pt[1 $\bar{1}$ 0] is indicated by the black arrow. The angle between the blue and black arrows is about 23°. **b** Zoomed-in STM image (U = 1 V, I = 0.05 nA) of the germanium adlayer. **c** Line profile along the dashed line in (**b**), revealing the periodicity of the germanium superstructure (1.2 nm). Reproduced with permission from Ref. [8], © 2014 Wiley

STM image of the germanium adlayer is displayed in Fig. 2.4b, demonstrating two other protrusions with different image contrast inside each supercell. Figure 2.4c shows the line profile along the dashed line of Fig. 2.4b, revealing that the periodicity of the brightest protrusions in the STM image is about 1.2 nm. This distance is equal to the dimension of ($\sqrt{19} \times \sqrt{19}$) superlattice of the Pt(111) surface; the lattice constant of Pt(111) is 0.277 nm ($\sqrt{19} \times 0.277$ nm = 1.21 nm). It is readily apparent that both the orientation and the periodicity of the germanium superstructure detected by STM are in good agreement with the analysis of the LEED pattern, confirming that a ($\sqrt{19} \times \sqrt{19}$) germanium superstructure was formed on the surface. In addition, the profile reveals a corrugation of around 0.6 Å in the germanium adlayer, indicating that different germanium atoms in the adlayer have different apparent heights with respect to the underlying Pt lattice, which we further analyzed using DFT calculations. This corrugation value is close to the buckled height (around 0.64 Å) of free-standing germanene in vacuum [1] and comparable to that of silicene on Ag(111) (0.75 Å) [14]. It implies that the Ge–Pt interaction is similar to the moderate Si–Ag interaction, which facilitates the formation of silicene on Ag(111).

Although Fig. 2.4b is not an STM image at atomic resolution, it is useful for one to construct an atomic model of the germanium adlayer. Note that the lattice constant of low-buckled free-standing germanene is about 3.97–4.02 Å based on the predictions of previous theoretical studies [1, 2, 15]. In that case, the lattice constant of the

(3 × 3) superlattice of the germanene is about 11.91–12.06 Å. This value is close to the periodicity (12 Å) of our observed structure, the ($\sqrt{19} \times \sqrt{19}$) germanium superstructure on Pt(111). Thus, we propose the following model to account for our observations: a single-layer germanene sheet is adsorbed on the Pt(111) surface at a certain rotation angle. As the rotation angle between the close-packed direction of Pt[1 $\bar{1}$ 0] and the ($\sqrt{19} \times \sqrt{19}$) germanium superstructure is determined to be about 23° (Fig. 2.4a), and the angle between the direction of the (1 × 1) lattice of germanene and the direction of its (3 × 3) superlattice is 0°, we can deduce the rotation angle of the high-symmetry direction of the germanium adlayer with respect to the substrate lattice, that is, about 23° between the (1 × 1) lattice of germanene and the Pt[1 $\bar{1}$ 0] direction. In this model, the ($\sqrt{19} \times \sqrt{19}$) supercell of the Pt(111) substrate nearly matches the (3 × 3) superlattice of the germanene sheet.

In order to obtain a detailed structural analysis of the germanium adlayer on Pt(111) and a deep understanding of the germanene/Pt(111) system, we calculated the geometric and electronic structures using DFT-based ab initio calculations, and we performed the corresponding STM simulations using the Tersoff-Hamann approach. Several models (different locations for the germanium atoms with respect to the substrate) were calculated. It turns out that the model with a honeycomb structure (germanene) shown in Fig. 2.5a (top view) is the most stable configuration. The binding energy of this configuration is about −1.39 eV per germanium atom. There are 18 germanium atoms per ($\sqrt{19} \times \sqrt{19}$) unit cell (the yellow rhombus). Different germanium atoms are situated in different chemical environments with respect to the Pt(111) surface. Such differences could account for the overall configuration of the germanene layer. The simulated STM image is shown in Fig. 2.5b, and one unit cell is indicated as a red rhombus. There are four protrusions at the vertices of the rhombus and two at the centers of the two triangular regions of the unit cell. These features are in excellent agreement with the STM observations in Fig. 2.4b, verifying that the model of the (3 × 3) germanene/($\sqrt{19} \times \sqrt{19}$) Pt(111) superstructure fundamentally resembles what we observed in our experiments. The relaxed model and the simulated STM image here provide a clear picture of the germanium arrangements in the

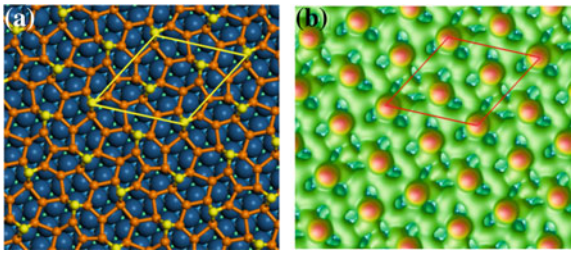

Fig. 2.5 **a** Top view of the relaxed atomic model of the (3 × 3) germanene/($\sqrt{19} \times \sqrt{19}$) Pt(111) configuration. The blue, yellow, and orange spheres represent Pt, protruding Ge, and other Ge atoms, respectively; a unit cell is outlined in yellow. **b** Simulated STM image, showing features identical with the experimental results. The brightness scale is represented by red > white > dark green, and a unit cell is outlined in red. Reproduced with permission from Ref. [8], © 2014 Wiley

adlayer observed in the actual STM images. The germanium atoms at the top sites of the underlying Pt atoms (the yellow spheres in Fig. 2.5a) correspond to the bright protrusions exhibited in the STM image (Fig. 2.4b). Furthermore, in the model, only one of the six germanium atoms in the honeycomb has a higher position, which differs from the theoretical models of a free-standing germanene sheet, wherein half of the germanium atoms have higher positions than the other half [1]. This suggests a substrate-induced buckled conformation of the germanene adlayer.

Although the germanene layer has a buckled structure with an undulation, it is a continuous layer rather than an accumulation of fragments with several germanium atoms, according to the analysis of the electron localization function (ELF). The ELF shows the charge localization between individual atoms, allowing us to appraise the chemical interaction between atoms directly. Figure 2.6a shows the top view of the overall ELF within the germanene layer with an ELF value of 0.5. Here, we see that chemical interaction exists between each pair of germanium atoms, showing the continuity of the germanene layer. This means the germanium atoms are well bonded to each other in the germanene sheet. In order to identify the bonding characteristics within each germanium pair clearly, the ELFs along the cross-section of each Ge–Ge pair (annotated in Fig. 2.6a) are displayed in Fig. 2.6b–f. The ELF values are shown by the color scheme, where red represents the electrons that are highly localized and blue signifies the electrons with almost no localization. It is clearly seen that electrons are localized to a large degree at the Ge–Ge pair containing a top-most Ge atom (the magnitudes of the ELF values are in the range of ~0.75–0.84, as shown in Fig. 2.6b, c, identifying a covalent bond between germanium atoms. The Ge–Ge pair (Fig. 2.6f) with the largest atomic distance has a slightly lower density of electrons localized in its intermediate location (ELF value is about 0.53). In conclusion, the ELFs presented here provide evidence that a covalent interaction exists between the members of each Ge–Ge pair. For comparison, the cross-section of the ELF between the germanium atom at the hexagonally close-packed (hcp) site and its nearest Pt atom is shown in Fig. 2.6g. The distance between such a Ge–Pt pair is the shortest one, and this is the position with the strongest interaction between the germanene layer and the substrate. However, the ELF value is only 0.29 in this case, much smaller than the ELF values of any of the germanium pairs. ELF values of less than 0.5 correspond to an absence of pairing between electrons. Therefore, it can be concluded that the interaction between germanium and the underlying platinum is mainly of an electrostatic origin. This interaction is not strong enough to affect the formation of Ge–Ge bonds and the extension of the germanium sheet. The evidence mentioned above demonstrates that a 2D continuous germanium layer—germanene—was indeed successfully fabricated on Pt(111).

It is worth noting, however, that a Ge–Pt substitutional surface alloy has been claimed previously by Ho et al. [16]. They annealed their sample at 900–1200 K to form a Ge–Pt surface alloy, aiming to obtain a longer catalyst lifetime. In their STM images, only four bright protrusions appear, located at the corners of each ($\sqrt{19} \times \sqrt{19}$) supercell. It is evident that their images show fewer features per unit cell than our high-resolution STM image (Fig. 2.4b). In their model, there is only one Ge atom within each ($\sqrt{19} \times \sqrt{19}$) supercell. This simple model is not suitable for our case,

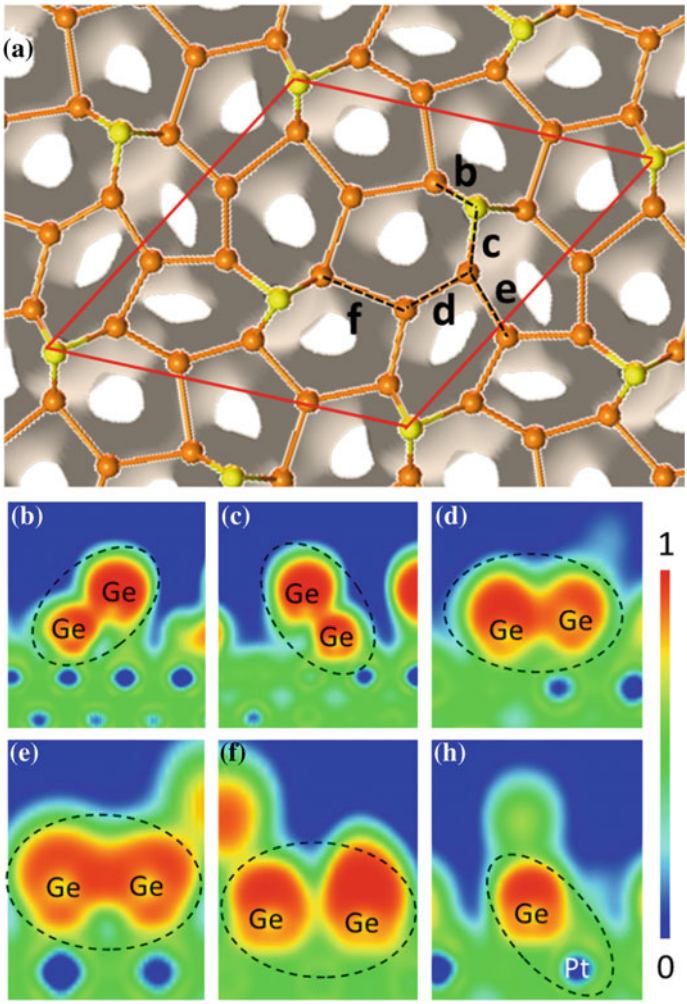

Fig. 2.6 **a** Top view of the overall electron localization function (ELF) of the relaxed model with an ELF value of 0.5, showing continuity of the germanene layer. Yellow and brown spheres represents Ge atoms, with the yellow spheres indicating the protruding Ge atoms. **b–f** The ELFs of the cross-sections between the germanium pairs indicated in (**a**), showing the covalent interaction existing between each pair of germanium atoms. The pairs are depicted by the dashed ovals. **g** The ELF of the cross section between one germanium atom and its nearest Pt neighbor. The ELF value here is in the range of the green-blue region (about 0.29), indicating an electrostatic interaction. The color scale for **b–g** is shown on the right. Reproduced with permission from Ref. [8], © 2014 Wiley

according to our theoretical simulations and experimental observations. We verified that the ($\sqrt{19} \times \sqrt{19}$) superstructure in our case originates not from Ge–Pt chemical contrast but instead from the charge density of state of the buckled germanene layer supported on Pt(111).

2.4 Summary and Outlook

We report for the first time on the fabrication of Ge-based graphene analog-germanene on a Pt(111) substrate.

(1) It features a ($\sqrt{19} \times \sqrt{19}$) superstructure related to the substrate lattice, as demonstrated by LEED and STM. Calculations based on first principles reveal that such a superstructure coincides with the (3×3) superlattice of a buckled germanene sheet.
(2) The calculated electron localization function shows that adjacent germanium atoms directly bind to each other, certifying the formation of a continuous 2D germanene sheet on the Pt(111) surface.
(3) This work provides a method of producing high-quality germanene on solid surfaces so as to explore its physical properties and potential applications in future functional nanodevices.

References

1. Cahangirov S, Topsakal M, Akturk E, Sahin H, Ciraci S (2009) Two- and one-dimensional honeycomb structures of silicon and germanium. Phys Rev Lett 102:236804. https://doi.org/10.1103/PhysRevLett.102.236804
2. Liu C-C, Feng W, Yao Y (2011) Quantum spin hall effect in silicene and two-dimensional germanium. Phys Rev Lett 107:076802
3. Baskaran G (2013) Silicene and germanene as prospective playgrounds for room temperature superconductivity. arXiv:1309.2242
4. Mannix AJ, Kiraly B, Hersam MC, Guisinger NP (2017) Synthesis and chemistry of elemental 2D materials. Nat Rev Chem 1:0014. https://doi.org/10.1038/S41570-016-0014
5. Bianco E et al (2013) Stability and exfoliation of germanane: a germanium graphane analogue. ACS Nano 7:4414–4421
6. Jiang SS et al (2014) Improving the stability and optical properties of germanane via one-step covalent methyl-termination. Nat Commun 5:3389. https://doi.org/10.1038/Ncomms4389
7. Jiang SS, Arguilla MQ, Cultrara ND, Goldberger JE (2015) Covalently-controlled properties by design in group IV graphane analogues. Acc Chem Res 48:144–151. https://doi.org/10.1021/ar500296e
8. Li LF et al (2014) Buckled germanene formation on Pt(111). Adv Mater 26:4820. https://doi.org/10.1002/adma.201400909
9. Gao M et al (2011) Epitaxial growth and structural property of graphene on Pt(111). Appl Phys Lett 98:033101. https://doi.org/10.1063/1.3543624
10. Gao M et al (2010) Tunable interfacial properties of epitaxial graphene on metal substrates. Appl Phys Lett 96:053109. https://doi.org/10.1063/1.3309671

11. Vanderbilt D (1990) Soft self-consistent pseudopotentials in a generalized eigenvalue formalism. Phys Rev B 41:7892
12. Kresse G, Furthmuller J (1996) Efficient iterative schemes for ab initio total-energy calculations using a plane-wave basis set. Phys Rev B 54:11169–11186. https://doi.org/10.1103/PhysRevB.54.11169
13. Perdew JP, Burke K, Ernzerhof M (1996) Generalized gradient approximation made simple. Phys Rev Lett 77:3865–3868. https://doi.org/10.1103/PhysRevLett.77.3865
14. Vogt P et al (2012) Silicene: compelling experimental evidence for graphenelike two-dimensional silicon. Phys Rev Lett 108:155501. https://doi.org/10.1103/PhysRevLett.108.155501
15. Lebegue S, Eriksson O (2009) Electronic structure of two-dimensional crystals from ab initio theory. Phys Rev B 79:115409
16. Ho CS, Banerjee S, Batzill M, Beck DE, Koel BE (2009) Formation and structure of a (root 19 x root 19)R23.4 degrees-Ge/Pt(111) surface alloy. Surf Sci 603:1161–1167. https://doi.org/10.1016/j.susc.2009.01.028